This MICCAI paper is the Open Access version, provided by the MICCAI Society. It is identical to the accepted version, except for the format and this watermark; the final published version is available on SpringerLink.

Variational Field Constraint Learning for Degree of Coronary Artery Ischemia Assessment

Qi Zhang[1], Xiujian Liu[1], Heye Zhang[1], Chenchu Xu[2], Guang Yang[3], Yixuan Yuan[4], Tao Tan[5], and Zhifan Gao[1] ⋆

[1] School of Biomedical Engineering, Sun Yat-sen University, Shenzhen, China
[2] Anhui University, Hefei, China
[3] Bioengineering Department and Imperial-X, Imperial College London, London, UK
[4] Department of Electronic Engineering, the Chinese University of Hong Kong, Hong Kong, China
[5] Macao Polytechnic University, Macao SAR

Abstract. Fractional flow reserve evaluation plays a crucial role in diagnosing ischemic coronary artery disease. Machine learning based fractional flow reserve evaluation has become the most important method due to it effectiveness and high computation efficiency. However, it still suffers from lacking of the proper description for the coronary artery fluid. This study presents a variational field constraint learning method for assessing fractional flow reserve from digital subtraction angiography images. Our method offers a promising approach by integrating governing equations and boundary conditions as unified constraints. By leveraging a holistic consideration of the fluid dynamics, our method achieves more accurate fractional flow reserve prediction compared to existing methods.

Keywords: machine learning · fractional flow reserve · hemodynamic · variational form

1 Introduction

Machine learning for assessing fractional flow reserve (FFR) stands out as a valuable approach in diagnosing ischemic coronary artery [1,2]. FFR is regarded as the gold standard in the functional diagnosis of coronary artery disease [3], due to its precise evaluation of the possibility of ischemia following stenosis. The FAME study, a landmark clinical trial, demonstrates a 4.5% reduction in mortality or myocardial infarction after 2 years under FFR guidance [4,5].However, the widespread adoption of FFR is hindered by medical instruments and diagnostic costs, prompting the use of various methods to evaluate FFR from images. Digital subtraction angiography, as a high-resolution imaging technique, furnishes critical information for the quantitative FFR assessment [6,7]. Computational fluid dynamics(CFD) and streamlined estimation methods gather geometric information from images and use numerical operation to calculate FFR. But those

⋆ Corresponding author. gaozhifan@gmail.com

two methods are limited by complex processing and accuracy [8]. Benefit from its computation efficiency and accuracy compared with other methods, machine learning-based FFR evaluation is considered as a promising method [9].

However, the machine learning-based FFR evaluation still encounters challenges. The challenge is difficult to build a unified description for the physical field [6]. The unified description of coronary fluid is challenging to establish, because it is difficult to find a paradigm to establish the relationship between Navier-Stokes equations and the boundary conditions [10]. Navier-Stokes equation defines the fundamental laws to control the flow of blood through the coronary artery[8]. The boundary conditions give the framework specific constraints[6]. Both of them depend on each other and work together to represent the dynamic of boundary-flowfield coupling. However, machine learning method faces challenge in predicting FFR, due to the lack of a suitable paradigm as a prior to describe the dynamic of boundary-flowfield coupling.

The existing methods are difficult to address the above challenge. Data-driven methods are hard to gather valuable features to predict FFR directly from images, due to ignore the fluid mechanics of coronary artery [10]. Apart from data-driven method, physics informed machine learning methods have considered the priors to tackle the challenges associated with data complexity. This progress is finished by integrating governing equation and boundary conditions separately [11,12]. However, separately learning these two constraints [13,14] and understanding one under the influence of the other [15,16] are hard to offer an effective solution to this challenge. Because they use a integral system as two distinct components, and it can introduce the mathematical instability and the inaccuracy in understanding the system's behavior.

In this study, we propose a variational field constraint learning method (VFCLM) to address the challenges associated with assessing FFR. VFCLM uses a variational form to constrain the learning process to obtain results consistent with physics. This variational form obtains a unified representation of the govern equations, inlet boundary condition and resistance boundary conditions by multi-domain fusion method[17], thereby ensuring precise prediction of FFR. The advantage of this method over the two separate constraints is it can more naturally integrate the governing equations and boundary conditions into a relatively concise and complete mathematical form [17]. This study introduces an elegant and robust mathematical structure, coupled with a corresponding multi-vessels network architecture.

The main contributions in the paper are four-fold:

1. We propose VFCLM to obtain physical information within the temporal and spatial domains of the coronary artery and accurately assess FFR from digital subtraction angiography images,
2. VFCLM introduces a variational form integrally taking into account the Navier-stokes equations and boundary conditions,
3. VFCLM uses a multi-vessel network structure and adds Murray's law as the hard constraint to satisfy the fluid properties in the vascular tree.

4. The extensive experiments on the 8000 synthetic coronary and digital subtraction imaging images of 180 cases. The performance of our VFCLM demonstrates the advantages over existing methods.

2 Method

2.1 Problem Statements

Previous related works used the Navier-Stokes equations and boundary conditions separately as the constraints and want to obtain physically consistent prediction of FFR [6,18,19], as shown in Fig. 1. However, considering boundary conditions and Navier-Stokes equations as separate constraints results in a system inconsistency and numerical instability. The Navier-Stokes equations and boundary conditions shape fluid fields. In physics-informed machine learning, they guide physical information calculation, but overlooking their interaction leads to issues in consistency, stability, and efficiency. This oversight complicates complex flow dynamics, especially in coronary FFR assessment.

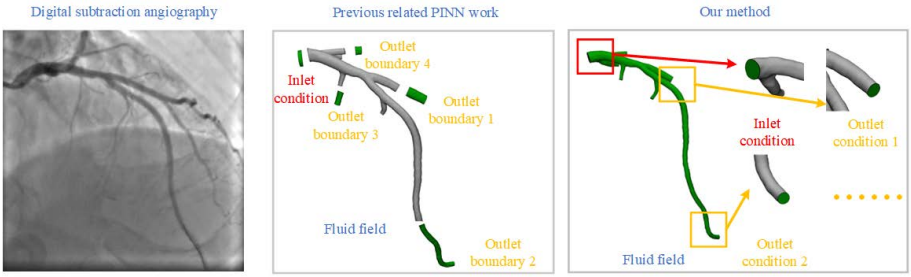

Fig 1. Previous related methods used boundary conditions and a fluid internal domain controlled by Navier-Stokes equations to describe the coronary artery, our approach takes it as a whole.

2.2 Variational Field Constraint Learning Method

In this study, we propose VFCLM for accurate FFR prediction from digital subtraction angiography images (Fig.2). We derive a variational form to consider Navier-Stokes equations and boundary conditions together, and use it as the constraint in multi-vessels neural network.

As shown in Fig.2, this VFCLM uses the coupling multi-domain method to describe the whole fluid field to predict the discrete distribution of flow and pressure. In details, coupling multi-domain methods are applied to the coupling of boundary and internal domains, and to the coupling of different vascular domains, respectively, to obtain predictions consistent with physics.

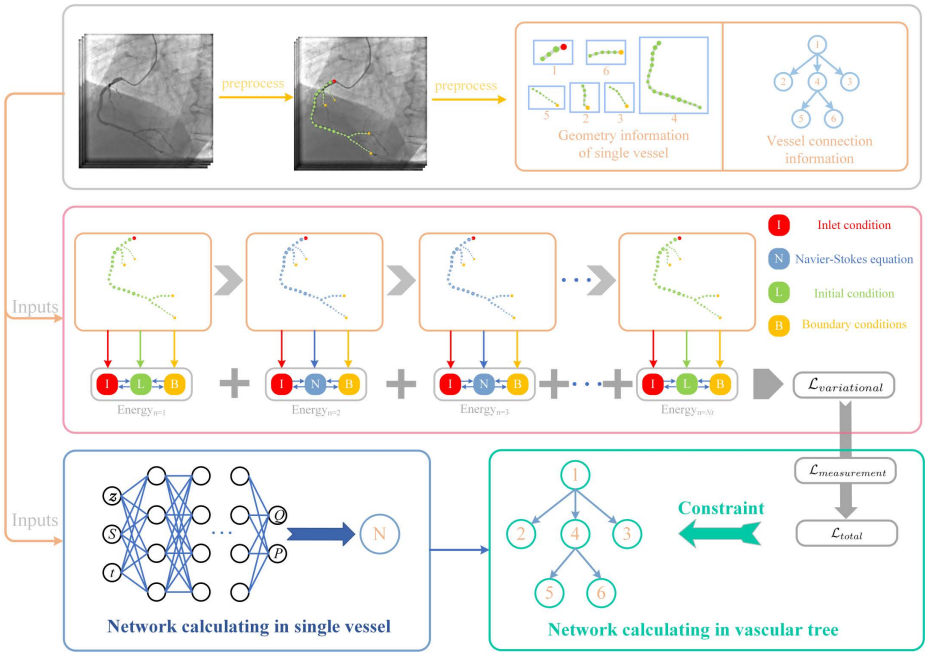

Fig 2. The schematics of the presented VFCLM framework.

Multi-vessels Neural Networks. In our study, we have implemented a prepossessing pipeline and utilized multi-vessels construction to calculate the physical information for multi-vessels. First, we extract geometric information from the image, which means the creation of an adjacency matrix representing the connectivity of blood vessels and path of the wave. According to this adjacency matrix we can effectively extract a top-down directed graph from it. This diagram determines the physical transmission of information between parents and child blood vessels (Murray's Law). Concurrently, we also extracted geometric parameters for each segment of the blood vessels. The combination of the adjacency matrix and the geometric data provides a comprehensive representation of the vascular network as shown in Fig.2. In details, we construct the corresponding single-vessel network according to the number of straight tubes, and determine the physical information transfer[9].

Derivation of Variational Form. During coronary FFR assessment, the Navier-Stokes equation can be simplified to a 1D form [19] as follow:

$$\frac{\partial Q}{\partial t}+\frac{4}{3}\frac{\partial}{\partial z}\left(\frac{Q^2}{S}\right)+\frac{S}{\rho}\frac{\partial P}{\partial z}=Sf-N\frac{Q}{S}+\frac{\mu}{\rho}\frac{\partial^2 Q}{\partial z^2},\quad z\in\Omega,t\in\mathbb{R}_{\geq 0} \tag{1}$$

$$\frac{\partial Q}{\partial z}+\frac{\partial S}{\partial t}=0,\quad z\in\Omega,t\in\mathbb{R}_{\geq 0} \tag{2}$$

this equation shows the interaction between the flow rate $Q(z,t)$, the pressure$P(z,t)$, and the cross-sectional area $S(z,t)$, the external force $f(z,t)$, along the vessel's centerline axial coordinate, z. By processing the clinical measurements, the inputs of VFCLM include the morphology $S(z) \in \mathbb{R}^{\mathbb{N}_v \times \mathbb{N}_d \times 1}$, the spatial coordinate $Z \in \mathbb{R}^{\mathbb{N}_v \times \mathbb{N}_d \times 1}$ and the boundary conditions $\gamma \in \mathbb{R}^{\mathbb{N}_b \times \mathbb{N}_t}$, as shown in Fig.2. The $\mathbb{N}_v$, $\mathbb{N}_b$, $\mathbb{N}_d$ and $\mathbb{N}_t$ are the number of vessel branches, sampling spatial points, coronary boundaries and sampling times points.

To simplify this problem, the arterial wall is considered as rigid without deformation, and gravitational effects are neglected, which represent the $S(z,t)$ can be replaced by $S(z)$ [20]. The inlet conditions are typically specified at begin of the 1D coronary artery[21]: $Q(z,t) = Q^{in}(t)$, where $z \in \mathcal{T}_{in}$.

Considering that Dirichlet boundary conditions are difficult to obtain, impedance boundary conditions $R(z)$ are adopted, and they are calculated by TIMI count method and Poiseuille equation [21,19]: $R(z) = P(z,t)/Q(z,t)$, where $z \in \mathcal{T}_{out}$.

In order to describe the coupling problem of multiple physical fields more clearly, we propose a quasi-linear conservative form [22] through (3) and (4) shown:

$$\frac{\partial U}{\partial t} + \frac{\partial F}{\partial z} - K\frac{\partial^2 U}{\partial z^2} = G \tag{3}$$

We define the details of the quasi-linear conservative form as followed:

$$\begin{aligned} U &= \begin{bmatrix} 0 \\ Q \end{bmatrix}, \quad F = \begin{bmatrix} Q \\ \frac{4}{3}\frac{Q^2}{S} + \frac{S}{\rho}\int_{P_0}^{P(z,t)} dP \end{bmatrix}, \\ K &= \begin{bmatrix} 0 & 0 \\ 0 & \nu \end{bmatrix}, \quad G = \begin{bmatrix} 0 \\ Sf + N\frac{Q}{S} + \int_{p_0}^{p} \frac{1}{\rho}\frac{\partial S(z)}{\partial z} dp \end{bmatrix} \end{aligned} \tag{4}$$

where the v represents the viscosity with value of $0.003Pas$, the details about N can be found in ref.[18].

In this research, we integrate the Navier-Stokes equations and boundary conditions into an variational form. This variational form provides a comprehensive framework for the generalized energy transformation across the entire fluid system. We use the Lagrange multiplier method to add the boundary condition as the part of the fluid system to provide the variational form[9]. Considering that the boundary condition is a pure impedance boundary, we bring the boundary condition into the energy functional. The variational form is given with range of $\Omega = [0, L]$ and $t = [0, T]$. The Lagrangian function is defined as $W = [W_1, W_2]$. Here, the description of the variational form in this system is defined as follow:

$$\begin{aligned} &\int_0^T \int_0^L \left(W_{,t}^T U + W_{,z}^T F - W_{,z}^T K U_{,z} + W^T G\right) dz dt \\ &+ \int_0^T W^T \left[F - KU_{,z} \right]_{z=0} dt - \int_0^T W^T \left[M(z) + H \right]_{z=L} dt \\ &+ \int_0^L W^T(z,T) U(z,T) dz - \int_0^L W^T(z,0) U^0(z) dz = 0 \end{aligned} \tag{5}$$

where the first part represents the Navier-Stokes equation, the second and third part represent the co-effects of the patient-specific inlet and outlet conditions with Navier-Stokes equation, the fourth and firth part define the co-effects of initial conditions with Navier-Stokes equations.And the $M_1(z) = p(z,t)/R(z)$, $M_2(z) = 4/3 * (M_1(z))^2/S$, $H_1(z) = H_2(z) = 0$.

Variational Energy Loss. For the purpose of effectively guiding and constraining the network training process with the variational form, we employed a stable space-time finite element method for its discretization[23].The discrete variational energy loss in single vessel is defined as follows:

$$\begin{aligned}\mathcal{L}_{variational} &= \frac{1}{N_d}\sum_{n=0}^{N_d-1}\sum_{m=0}^{N_t-1} W^{n,m}\left[U^{n,m+1} - M^{n,m}\right] \\ &+ \frac{\Delta t}{(N_d-1)(N_t-1)}\sum_{n=1}^{N_d-1}\sum_{m=1}^{N_t-1}(W_z^{n,m}F^{n,m} - W_{.z}^{n,m}KU_{.z}^{n,m} + W^{n,m}G^{n,m}) \\ &+ \frac{\Delta t}{N_t}\sum_{m=0}^{N_t-1} W^{0,m}F^{0,m} - \frac{\Delta t}{N_t}\sum_{m=0}^{N_t-1} W^{N_d,m}F^{N_d,m}\end{aligned} \tag{6}$$

Measurements Loss. A potential issue with the variational form is that it may lead the network to converge towards the true solution in various directions. To address this, we incorporate the discrepancy between actual measurements and predicted values as a component of the loss function. The measurement loss can be described as follow:

$$\mathcal{L}_{measurement} = \sqrt{\frac{1}{N_c}\sum_{c=1}^{N_c}(Q^{n,m} - Q^{n,m,c})^2} \tag{7}$$

where the N_c defines the number of measurement points, the $Q^{n,m,c}$ represents the clinical measurements or computational fluid mechanics simulation results of the n^{th} point at m^{th} time.

Total Loss. The total loss can be calculated by the variational energy loss and measurements loss, which can be written as:$\mathcal{L}_{total} = \mathcal{L}_{variational} + \mathcal{L}_{measurement}$.

Through this variational constraint, we can uniformly consider the governing equations and boundary conditions of coronary artery to obtain accurate FFR prediction.

3 Experiments and Results

3.1 Materials and Experiments Setup

In this research, We use two types of datasets in experiments, including 8000 virtual coronary artery trees building by 0D-1D hemodynamic coronary tree models

and 180 digital subtraction angiography images from patients.In all experiments, the Adam optimizer is used with 16 batch size per step. Initial learning rate is 0.001 and the decay rate is 0.95.

When constructing the virtual subject dataset, we systematically varied parameters within a reasonable range, such as boundary conditions, intravascular geometry, and vessel length etc. Moreover, this virtual subjects have been fed into 0D-1D hemodynamic model to obtain the physical information of the coronary artery [24].

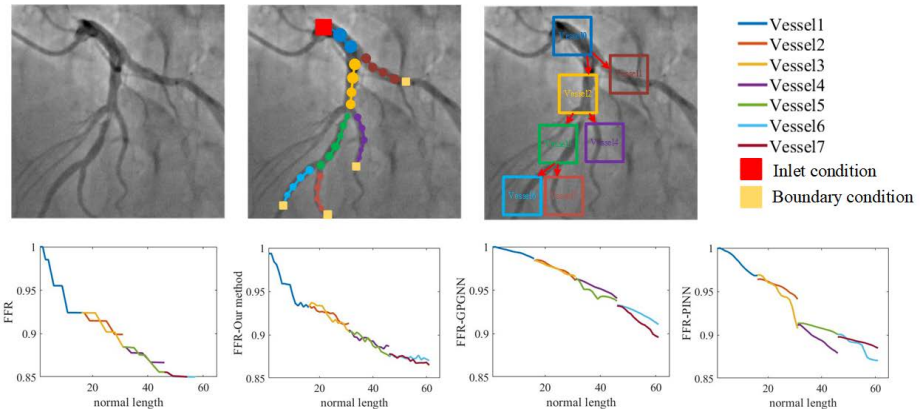

Fig 3. The comparison of our method with PINN and GPGNN in virtual dataset in one case.

In the in-vivo dataset, digital subtraction angiography images were obtained from 180 patients who provided informed consent, adhering to clinical standards. FFR measurements were conducted using a pressure guide-wire (Abbott, model HI-TORQUE). Inlet conditions $Q_{in}(t)$ were represented as waveforms proportional to vessel inlet diameter, with single resistance boundary conditions $R(z)$ calculated using the Poiseuille equation. VFCLM was compared against four state-of-the-art methods: PINN, GPGNN, and 1D-CFD and 0D-CFD models. Evaluation metrics included Mean Absolute Errors (MAE) and Mean Absolute Percentage Errors (MAPE), measured in mmHg and

Results on Virtual Dataset.In the virtual dataset, VFCLM outperformed other methods, including CFD, as indicated in Table 1 and Fig. 3. The physics-informed neural network exhibited poor performance on unseen coronary due to the separate consideration of governing equations and boundary conditions. This separation led to incomplete utilization of available information, affecting the accuracy of predictions.

Results on In-vivo Dateset.In the in-vivo dataset, VFCLM demonstrated superior performance compared to other methods, including CFD, as illustrated in Table 1 and Fig. 4. Notably, we included CFD results for comparison purposes, as relying solely on physics-based constraints poses limitations in achieving ac-

curate predictions. Our findings reveal that VFCLM outperforms hemodynamic simulations, attributed to its utilization of a weak form to guide the network and incorporate $\mathcal{L}_{measurement}$ for convergence towards clinical measurements. Consequently, VFCLM achieves higher accuracy in generating realistic coronary physical information distributions than CFD.

Table 1. Comparison of our method and four advanced methods for pressure prediction on virtual and in-vivio dataset. LAD, left anterior descending artery; LCX, left circumflex artery; RCA, right coronary artery.

		our		PINN		GPGNN		1D-CFD		0D-CFD	
		MAE	MAPE	MAE	MAPE	MAE	MAPE	MAE	MAPE	MAE	MAPE
Virtual	LAD	**0.79**	**0.87**	1.79	2.03	1.07	1.21	-	-	-	-
	RCA	**0.87**	**1.04**	2.45	2.72	1.38	1.27	-	-	-	-
dataset	LCX	**1.24**	**1.51**	1.54	1.29	1.20	1.11	-	-	-	-
In-vivo	LAD	**1.09**	**0.99**	2.78	2.94	1.54	1.71	1.44	1.37	1.49	1.54
	RCA	**0.70**	**0.67**	2.93	3.02	1.84	1.90	1.38	1.39	1.71	1.68
dataset	LCX	**1.18**	**1.27**	2.69	2.90	1.87	1.98	1.81	1.96	2.70	2.47

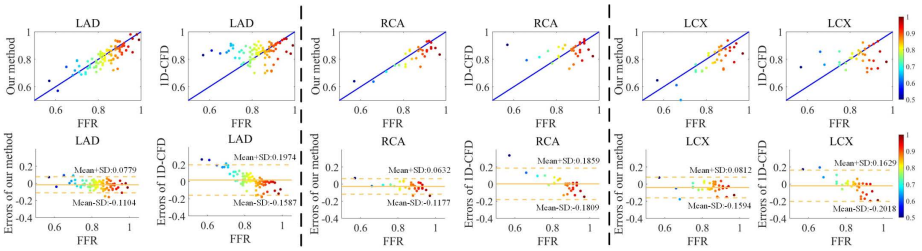

Fig 4. The comparison of our method with 1D hemodynamics simulation in in-vivo dataset. The FFR represents the clinical measurement which is used as ground truth in in-vivo dataset. The 1D-FFR represents the results of 1D hemodynamic models.

4 Conclusion

In this research, we propose a variational field constraint learning method (VFCLM) to evaluate the FFR from digital subtraction angiography images. VFCLM overcomes the current limitations of machine learning in the gradient descent and system consistencies. The rationale behind this lies in VFCLM's holistic constraint, which integrates governing equations and variational boundary conditions as unified part. Whether compared with other machine learning methods or computational fluid dynamics methods, this method shows advan-

tages, which means that this method has the potential to be applied in clinical practice.

Acknowledgments

This work was supported in part by The National Key Research and Development Program of China (2022YFE0209800), Shenzhen Science and Technology Program (GJHZ20220913142601003), National Natural Science Foundation of China (62101606, 62276282, 62101610, 62325113, 62271511), Guangdong Basic and Applied Basic Research Foundation (2024B1515020062, 2022A1515011384).

Disclosure of Interests

The authors have no competing interests to declare that are relevant to the content of this article.

References

1. Yuehua Li, Mengmeng Yu, Xu Dai, Zhigang Lu, Chengxing Shen, Yining Wang, Bin Lu, and Jiayin Zhang. Detection of hemodynamically significant coronary stenosis: Ct myocardial perfusion versus machine learning ct fractional flow reserve. *Radiology*, 293(2):305–314, 2019.
2. Zhifan Gao, Xin Wang, Shanhui Sun, Dan Wu, Junjie Bai, Youbing Yin, Xin Liu, Heye Zhang, and Victor Hugo C de Albuquerque. Learning physical properties in complex visual scenes: An intelligent machine for perceiving blood flow dynamics from static ct angiography imaging. *Neural Networks*, 123:82–93, 2020.
3. PIJLS NH. Fractional flow reserve: A useful index to evaluate the influence of an epicardial coronary stenosis on myocardial blood flow. *Circulation*, 92:3183–3193, 1995.
4. Bernard de Bruyne, Jozef Bartunek, Stanislas U Sys, Nico HJ Pijls, Guy R Heyndrickx, and William Wijns. Simultaneous coronary pressure and flow velocity measurements in humans: feasibility, reproducibility, and hemodynamic dependence of coronary flow velocity reserve, hyperemic flow versus pressure slope index, and fractional flow reserve. *Circulation*, 94(8):1842–1849, 1996.
5. Nico HJ Pijls, William F Fearon, Pim AL Tonino, Uwe Siebert, Fumiaki Ikeno, Bernhard Bornschein, Marcel van't Veer, Volker Klauss, Ganesh Manoharan, Thomas Engstrøm, et al. Fractional flow reserve versus angiography for guiding percutaneous coronary intervention in patients with multivessel coronary artery disease: 2-year follow-up of the fame (fractional flow reserve versus angiography for multivessel evaluation) study. *Journal of the American College of Cardiology*, 56(3):177–184, 2010.
6. Baihong Xie, Xiujian Liu, Heye Zhang, Chenchu Xu, Tieyong Zeng, Yixuan Yuan, Guang Yang, and Zhifan Gao. Conditional physics-informed graph neural network for fractional flow reserve assessment. In *International Conference on Medical Image Computing and Computer-Assisted Intervention*, pages 110–120. Springer, 2023.

7. Charles A Taylor, Kersten Petersen, Nan Xiao, Matthew Sinclair, Ying Bai, Sabrina R Lynch, Adam UpdePac, and Michiel Schaap. Patient-specific modeling of blood flow in the coronary arteries. *Computer Methods in Applied Mechanics and Engineering*, 417:116414, 2023.
8. Christian Tesche, Carlo N De Cecco, Stefan Baumann, Matthias Renker, Tindal W McLaurin, Taylor M Duguay, Richard R Bayer 2nd, Daniel H Steinberg, Katharine L Grant, Christian Canstein, et al. Coronary ct angiography–derived fractional flow reserve: machine learning algorithm versus computational fluid dynamics modeling. *Radiology*, 288(1):64–72, 2018.
9. Leonardo Chirco and Sandro Manservisi. An adjoint based pressure boundary optimal control approach for fluid-structure interaction problems. *Computers & Fluids*, 182:118–127, 2019.
10. Hyeonyong Hae, Soo-Jin Kang, Won-Jang Kim, So-Yeon Choi, June-Goo Lee, Youngoh Bae, Hyungjoo Cho, Dong Hyun Yang, Joon-Won Kang, Tae-Hwan Lim, et al. Machine learning assessment of myocardial ischemia using angiography: Development and retrospective validation. *Plos Medicine*, 15(11):e1002693, 2018.
11. Sifan Wang, Hanwen Wang, and Paris Perdikaris. Learning the solution operator of parametric partial differential equations with physics-informed deeponets. *Science Advances*, 7(40):eabi8605, 2021.
12. Georgios Kissas, Yibo Yang, Eileen Hwuang, Walter R Witschey, John A Detre, and Paris Perdikaris. Machine learning in cardiovascular flows modeling: Predicting arterial blood pressure from non-invasive 4d flow mri data using physics-informed neural networks. *Computer Methods in Applied Mechanics and Engineering*, 358:112623, 2020.
13. Xuelan Zhang, Baoyan Mao, Yue Che, Jiaheng Kang, Mingyao Luo, Aike Qiao, Youjun Liu, Hitomi Anzai, Makoto Ohta, Yuting Guo, et al. Physics-informed neural networks (pinns) for 4d hemodynamics prediction: An investigation of optimal framework based on vascular morphology. *Computers in Biology and Medicine*, 164:107287, 2023.
14. Mohammad Sarabian, Hessam Babaee, and Kaveh Laksari. Physics-informed neural networks for brain hemodynamic predictions using medical imaging. *IEEE Transactions on Medical Imaging*, 41(9):2285–2303, 2022.
15. Nadim Saad, Gaurav Gupta, Shima Alizadeh, and Danielle C Maddix. Guiding continuous operator learning through physics-based boundary constraints. *arXiv preprint arXiv:2212.07477*, 2022.
16. Henrik Rosenberger and Benjamin Sanderse. No pressure? energy-consistent roms for the incompressible navier-stokes equations with time-dependent boundary conditions. *Journal of Computational Physics*, 491:112405, 2023.
17. Luca Pegolotti, Martin R Pfaller, Alison L Marsden, and Simone Deparis. Model order reduction of flow based on a modular geometrical approximation of blood vessels. *Computer Methods in Applied Mechanics and Engineering*, 380:113762, 2021.
18. Martin R Pfaller, Jonathan Pham, Aekaansh Verma, Luca Pegolotti, Nathan M Wilson, David W Parker, Weiguang Yang, and Alison L Marsden. Automated generation of 0d and 1d reduced-order models of patient-specific blood flow. *International Journal for Numerical Methods in Biomedical Engineering*, 38(10):e3639, 2022.
19. Qi Zhang, Yahui Zhang, Liling Hao, Yujia Zhong, Kunlin Wu, Zhuo Wang, Shuai Tian, Qi Lin, and Guifu Wu. A personalized 0d-1d model of cardiovascular system for the hemodynamic simulation of enhanced external counterpulsation. *Computer Methods and Programs in Biomedicine*, 227:107224, 2022.

20. Cheong-Ah Lee, Hafiz Muhammad Umer Farooqi, and Dong-Guk Paeng. Axial shear rate: A hemorheological factor for erythrocyte aggregation under womersley flow in an elastic vessel based on numerical simulation. *Computers in Biology and Medicine*, 157:106767, 2023.
21. Umberto Morbiducci, Raffaele Ponzini, Diego Gallo, Cristina Bignardi, and Giovanna Rizzo. Inflow boundary conditions for image-based computational hemodynamics: impact of idealized versus measured velocity profiles in the human aorta. *Journal of Biomechanics*, 46(1):102–109, 2013.
22. Luca Pegolotti, Martin R Pfaller, Alison L Marsden, and Simone Deparis. Model order reduction of flow based on a modular geometrical approximation of blood vessels. *Computer Methods in Applied Mechanics and Engineering*, 380:113762, 2021.
23. H Huang and F Costanzo. On the use of space–time finite elements in the solution of elasto-dynamic problems with strain discontinuities. *Computer Methods in Applied Mechanics and Engineering*, 191(46):5315–5343, 2002.
24. Paul D Morris, Andrew Narracott, Hendrik von Tengg-Kobligk, Daniel Alejandro Silva Soto, Sarah Hsiao, Angela Lungu, Paul Evans, Neil W Bressloff, Patricia V Lawford, D Rodney Hose, et al. Computational fluid dynamics modelling in cardiovascular medicine. *Heart*, 102(1):18–28, 2016.